

2

TECHNICAL REPORT BRL-TR-3132

BRL

AD-A228 137

TUNNEL-EXIT PRESSURE AND IMPULSE EFFECTS
ON FREE-FIELD PRESSURE AND IMPULSE

CHARLES N. KINGERY
EDMUND J. GION

AUGUST 1990

DTIC
ELECTE
OCT 30 1990
S E D
lc

APPROVED FOR PUBLIC RELEASE; DISTRIBUTION UNLIMITED.

U.S. ARMY LABORATORY COMMAND

BALLISTIC RESEARCH LABORATORY
ABERDEEN PROVING GROUND, MARYLAND

NOTICES

Destroy this report when it is no longer needed. DO NOT return it to the originator.

Additional copies of this report may be obtained from the National Technical Information Service, U.S. Department of Commerce, 5285 Port Royal Road, Springfield, VA 22161.

The findings of this report are not to be construed as an official Department of the Army position, unless so designated by other authorized documents.

The use of trade names or manufacturers' names in this report does not constitute indorsement of any commercial product.

UNCLASSIFIED

REPORT DOCUMENTATION PAGE			Form Approved OMB No. 0704-0188
Public reporting burden for the collection of information is estimated to average 1 hour per response, including the time for reviewing instructions, searching existing data sources, gathering and maintaining the data needed, and completing and reviewing the collection of information. Send comments regarding this burden estimate or any other aspect of this collection of information, including suggestions for reducing this burden, to Washington Headquarters Services, Directorate for Information Operations and Reports, 1215 Jefferson Davis Highway, Suite 1204, Arlington, VA 22202-4302, and to the Office of Management and Budget, Paperwork Reduction Project (0704-0188), Washington, DC 20503			
1. AGENCY USE ONLY (Leave blank)	2. REPORT DATE AUGUST 1990	3. REPORT TYPE AND DATES COVERED Final, Jan 88 - Jan 89	
4. TITLE AND SUBTITLE Tunnel-Exit Pressure and Impulse Effects on Free-Field Pressure and Impulse		5. FUNDING NUMBERS PR: P665 805M857	
6. AUTHOR(S) Charles N. Kingery and Edmund J. Gion			
7. PERFORMING ORGANIZATION NAME(S) AND ADDRESS(ES)		8. PERFORMING ORGANIZATION REPORT NUMBER	
9. SPONSORING / MONITORING AGENCY NAME(S) AND ADDRESS(ES) US Army Ballistic Research Laboratory ATTN: SLCBR-DD-T Aberdeen Proving Ground, MD 21005-5066		10. SPONSORING / MONITORING AGENCY REPORT NUMBER BRL-TR-3132	
11. SUPPLEMENTARY NOTES			
12a. DISTRIBUTION / AVAILABILITY STATEMENT Approved for public release; distribution unlimited.		12b. DISTRIBUTION CODE	
13. ABSTRACT (Maximum 200 words) This report presents the results of a series of experimental tests conducted to determine the effect of the overpressure vs. time history exiting a shock tube on the peak overpressure and impulse produced outside of the tube. A 2.54-cm-diameter shock tube was used with a 22.86-cm driver section and a 133-cm driven section to produce a short-duration, decaying, pressure-time pulse at the exit end of the tube. Seven transducer locations recorded the peak overpressure and overpressure impulse vs. time along the zero-degree line. A second series of tests was conducted using a 150-cm driver to produce a long-duration, flattop, pressure-time pulse at the exit end of the tube. Again the overpressure vs. time was recorded at selected distances for comparison with the short driver results. It was determined that the flattop, longer duration, exit-pressure pulses produce higher pressure ratios, $\Delta P/P_w$, for the same distance ratio, R/D_T , than the short-duration, decaying pressure pulse at R/D_T greater than 10. It was determined that, to correlate the impulse I_s outside of the tube with the exit impulse I_e , it was necessary to scale both I_s and R/D_T by dividing each by I_w raised to the 1/3 power (i.e., $(I_w)^{1/3}$). The effect of the exiting wave shape would have some influence on the present or proposed quantity-distance safety criteria.			
14. SUBJECT TERMS Airblast; Underground Storage; Impulse; Blast Waves; Tunnel Exit Pressure; Blast Propagation; Quantity Distance		15. NUMBER OF PAGES 42	
		16. PRICE CODE	
17. SECURITY CLASSIFICATION OF REPORT UNCLASSIFIED	18. SECURITY CLASSIFICATION OF THIS PAGE UNCLASSIFIED	19. SECURITY CLASSIFICATION OF ABSTRACT UNCLASSIFIED	20. LIMITATION OF ABSTRACT UL

INTENTIONALLY LEFT BLANK.

TABLE OF CONTENTS

	<u>Page</u>
LIST OF FIGURES	v
LIST OF TABLES	vii
1 INTRODUCTION	1
1.1 Background	1
1.2 Objectives	1
2 TEST PROCEDURES	1
2.1 Shock Tube Description	1
2.2 Instrumentation Description	3
2.3 Transducer Locations	3
3 RESULTS	3
3.1 Peak Overpressure vs. Distance--Decaying Exit Pressure	3
3.2 Peak Overpressure vs. Distance--Flattop Exit Pressure	7
3.3 Impulse vs. Distance--Decaying Exit Pressure	7
3.4 Impulse vs. Distance--Flattop Exit Pressure	15
4 CONCLUSIONS	19
5 REFERENCES	21
APPENDIX: DATA FROM DETONATIONS OF HIGH EXPLOSIVE IN MUNITION STORAGE MODELS	23
DISTRIBUTION LIST	33

Accession For	
WEIS GRA&I	<input checked="" type="checkbox"/>
DTIC TAB	<input type="checkbox"/>
Unannounced	<input type="checkbox"/>
Justification	
By _____	
Distribution/	
Availability Codes	
Dist	Avail and/or Special
A-1	



INTENTIONALLY LEFT BLANK.

LIST OF FIGURES

<u>Figure</u>	<u>Page</u>
1. Shock Tube and Field Test Configurations	2
2. Schematic of Data Acquisition-Reduction System	4
3. Pressure Ratio $\Delta P/P_w$ vs. Distance Ratio R/D_T for a Short-Duration, Decaying Exit-Pressure Shockwave	6
4. Tunnel-Exit Overpressure vs. Time for a Shock Tube Flattop and Decaying Wave Forms and a High-Explosive, Test Model, Decaying Wave	8
5. Pressure Ratio $\Delta P/P_w$ vs. Distance Ratio R/D_T for a Flattop and Long-Duration, Decaying Pressure Pulse	10
6. Impulse Ratio I_s/I_w vs. Distance Ratio R/D_T for a Short-Duration, Decaying Exit-Pressure Pulse	12
7. Scaled Impulse vs. Scaled Distance Ratio for Short-Duration, Decaying Exit-Pressure Pulses	14
8. Measured Impulse I_s vs. Distance Ratio R/D_T for Three Flattop Exit-Impulse Ranges	16
9. Scaled Impulse vs. Scaled Distance Ratio for Flattop, Exit-Pressure Pulses	18
A-1. Pressure Ratio $\Delta P/P_w$ vs. Distance Ratio R/D_T (from Reference 2)	27
A-2. Pressure Ratio $\Delta P/P_w$ vs. Distance Ratio R/D_T (from Reference 6)	29
A-3. Scaled Impulse $I_s/I_w^{1/3}$ vs. Scaled Distance Ratio $(R/D_T)/(I_w)^{1/3}$ (from References 2 and 6)	31

INTENTIONALLY LEFT BLANK.

LIST OF TABLES

<u>Table</u>	<u>Page</u>
1. Side-On Peak Pressure and Impulse Along the Zero-Degree Line--Short-Duration, Decaying Exit Wave	5
2. Side-On Peak Pressure and Impulse Along the Zero-Degree Line--Long-Duration, Flattop Exit Wave	9
3. Side-On Scaled Impulse and Scaled Distance Ratio for Short-Duration, Decaying Exit Wave	13
4. Side-On Scaled Impulse and Scaled Distance Ratio for a Flattop Exit Wave	17
A-1. Peak Overpressure and Impulse Data	26
A-2. Peak Overpressure and Impulse Data	28

INTENTIONALLY LEFT BLANK.

1. INTRODUCTION

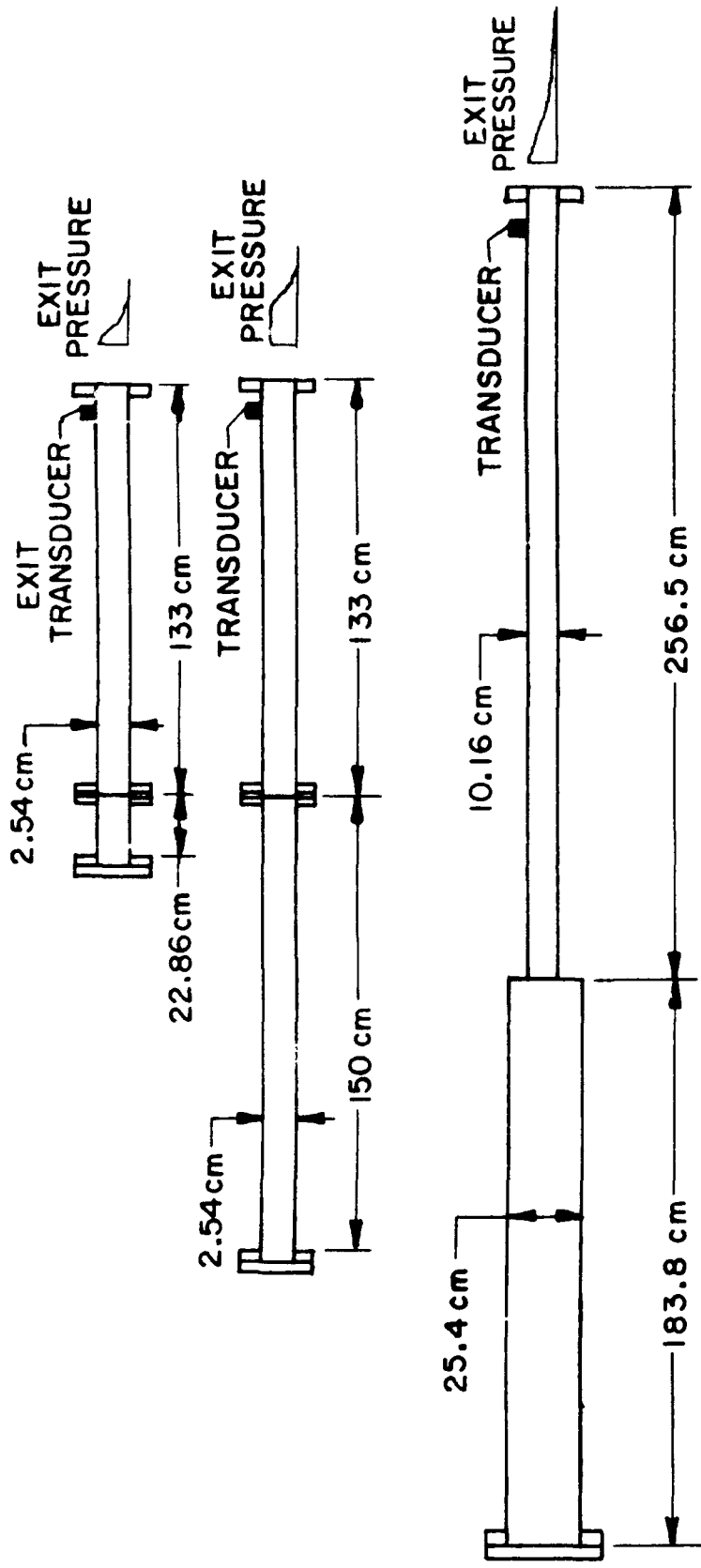
1.1 Background. One of the missions of the Department of Defense Explosives Safety Board (DDESB) is the characterization of airblast effects relative to structural damage in order to establish quantity-distance (Q-D) standards for ordnance used by the armed services. The present published safety manual (Ammunition and Explosives Safety Standards) has many tables establishing the safe distances for various types of buildings and equipment. These distances are based on the amount of explosive stored and how it is stored (i.e., in the open with barricades, in earth-covered magazines, or in underground storage sites). The Q-D criteria established for explosives stored in *underground storage sites* are based on the distance at which a given peak overpressure would accrue from known quantities of explosive. The point to be made here is that only the peak overpressure is considered and not the duration of the overpressure or the impulse of the pressure pulse.

1.2 Objectives. The general objectives of this research project is to experimentally investigate the relationship, if any, between the side on overpressure wave shape and impulse exiting a shock tube or underground storage tunnel and the peak side-on overpressure recorded at selected distances in front of the tube exit.

A second objective is to determine what relationship exists between the exit-pressure wave shape and side-on overpressure impulse exiting the shock tube, and the side-on impulse recorded at selected distances in front of the tube exit.

2. TEST PROCEDURES

2.1 Shock Tube Description. The experimental phase of this project was conducted in a large, enclosed area with a controlled environment. A 2.54-cm inside diameter shock tube was selected for use because it could be operated indoors without resorting to remote control. To look at the effect of changing the exiting overpressure impulse, the length of the driver section was varied. The driver section was 22.86 cm in length to produce a decaying shock wave at the exit of a 133-cm driven section. To produce a flattop-type shock wave at the tube exit, a driver section of 150 cm in length was used with a 133-cm-length driven section. A sketch of the two shock tube configurations is shown in Figure 1, as well as a field test model. Results from those tests will also be compared with the shock tube tests.



NOT TO SCALE

Figure 1. Shock Tube and Field Test Configurations.

2.2 Instrumentation Description. A schematic of the data acquisition-reduction system is given in Figure 2. Quartz piezoelectric transducers were used to record the side-on overpressure vs. time, from which impulse vs. time can be calculated. The transducers are coupled through a power supply and data amplifiers to a digitizing oscilloscope. On-site comparisons of the results were made directly from the hard copies of the pressure-vs.-time records. Final data processing and generation of the overpressure and overpressure impulse vs. time were completed with the computer, printer, and plotter.

2.3 Transducer Locations. The pressure transducers were located at selected distances from the shock tube exit. The inside diameter of the tube is 2.54 cm, and because the decay of peak overpressure appears to be a function of the ratio of distance from the tube exit (R) divided by the tube diameter D_T , the locations are listed in units of tube diameters. There were eight locations along the zero line. They were 4.5, 6.5, 10, 15, 23, 35, 54 and 100 diameters. The distances can be read directly in inches or multiplied by 2.54 to be read in centimeters.

3. RESULTS

3.1 Peak Overpressure vs. Distance-Decaying Exit Pressure. One of the objectives of this project is to determine whether the shape of the overpressure pulse has influence on the decay of peak overpressure vs. distance outside of the shock tube. The peak overpressure recorded at the transducer stations outside of the shock tube are listed in Table 1 for the 22.86-cm driver. The peak overpressures, AP, are listed in units of kPa and also as ratios of AP divided by the exit pressure P_w . These values are plotted in Figure 3 to determine how well they fit an equation from Reference 4 (Kingery 1989), which was developed by the Norwegians (Skjeltrojs, Jensen, and Rinuan 1977). The equation is:

$$AP/P_w = 1.24 (R/D_T)^{1.15} / (1 + (0/56)^2), \quad (1)$$

where AP/P_w is the free-field-blast-pressure-to-exit-pressure ratio found at a radial-distance-to-tunnel-diameter ratio R/D_T and 0 degrees from the tunnel exit. The data presented in Table 1 are taken along the zero degree line, and, therefore, only the first part of Equation 1 is used.

The peak overpressure data listed in Table 1 are presented in graphical form in Figure 3 as AP/P_w vs. R/D_T . The solid line was calculated from Equation 1, and, as can be seen, the scatter of data from the recorded pressure vs. time records is quite acceptable. The only trend noted is that

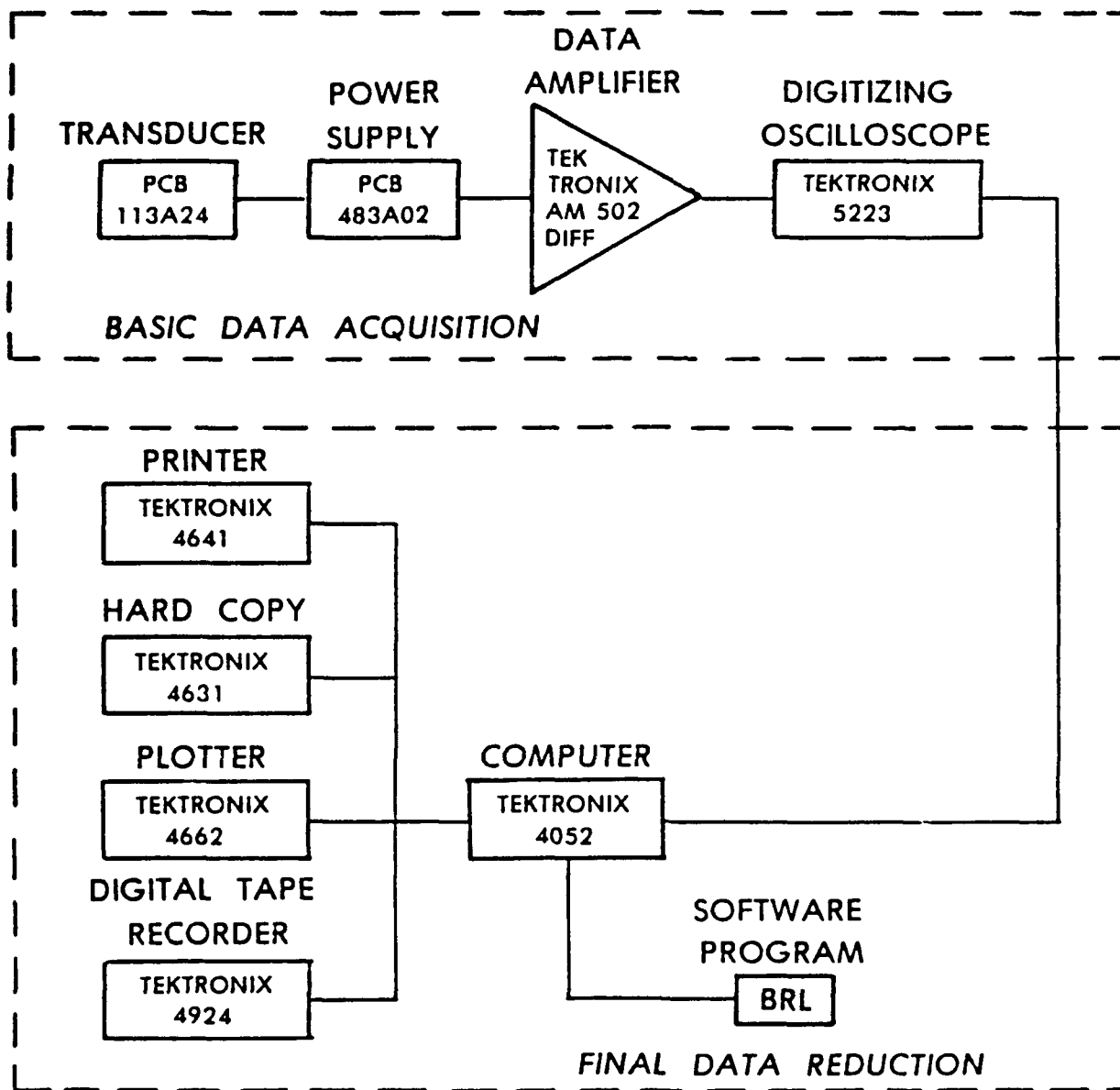


Figure 2. Schematic of Data Acquisition-Reduction System.

TABLE 1. Side-On Peak Pressure and Impulse Along the Zero-Degree Line--Short-Duration, Decaying Exit Wave.

Test no.	Distance ratio, R/D_T	P_w , kPa	ΔP , kPa	Pressure ratio, $\Delta P/P_w$	I_w , kPa -msec	I_s , kPa -msec	Impulse ratio, $\Delta I_s/I_w$
16	4.5	478	8.15	0.0171	284	24.80	0.0870
16	6.5	478	40.2	0.0840	284	14.70	0.0520
16	10.0	478	21.8	0.0460	284	6.84	0.0240
17	15.0	491	13.5	0.0270	242	4.00	0.0160
16	23.0	478	6.6	0.0140	284	1.90	0.0067
17	35.0	491	3.1	0.0063	242	0.72	0.0030
17	54.0	491	2.3	0.0047	242	0.50	0.0021
8	4.5	747	99.9	0.1340	606	20.80	0.0340
8	6.5	747	74.7	0.1000	606	17.50	0.0290
19	10.0	654	36.5	0.0560	504	13.10	0.0260
19	15.0	654	27.3	0.0420	504	7.36	0.0150
8	23.0	747	14.5	0.0190	606	6.10	0.0100
19	35.0	654	6.4	0.0098	504	1.35	0.0027
19	54.0	654	3.6	0.0055	504	--	--
21	6.5	1,196	171.0	0.1430	1,356	27.70	0.0200
21	10.0	1,196	78.7	0.0660	1,356	21.80	0.0160
20	15.0	1,222	47.7	0.0390	1,392	16.30	0.0120
21	23.0	1,196	24.2	0.0200	1,356	11.90	0.0088
20	35.0	1,222	10.6	0.0087	1,392	4.61	0.0033
20	54.0	1,222	8.0	0.0065	1,392	2.64	0.0019
20	100.0	1,222	3.1	0.0025	1,392	1.21	0.0014

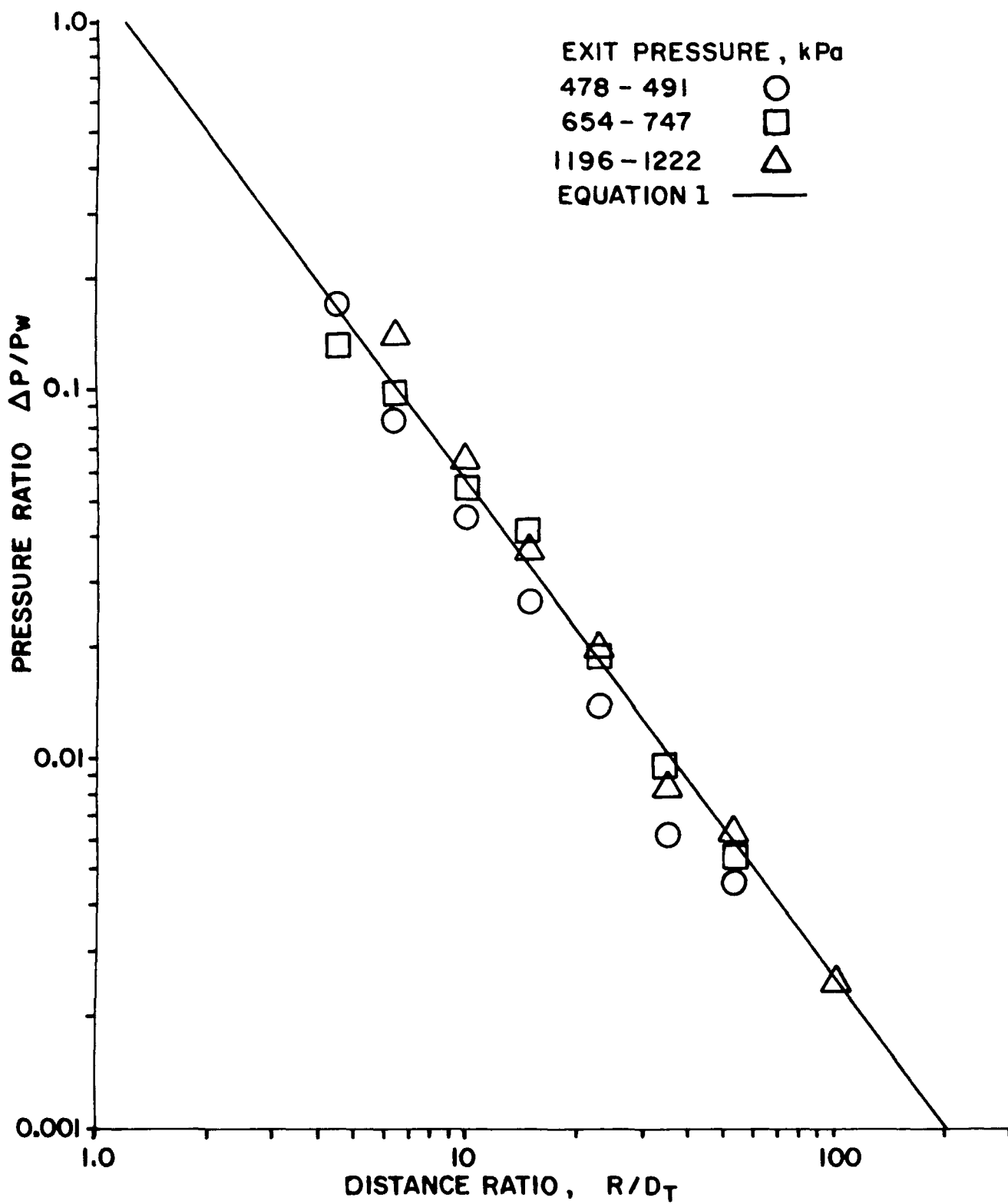


Figure 3. Pressure Ratio $\Delta P/P_w$ vs. Distance Ratio R/D_T for a Short-Duration, Decaying Exit-Pressure Shockwave.

the ratios from the lower exit pressure (478 - 491 kPa) fall below the solid line with one exception. The mid-level exit pressure (654 - 747 kPa) and the upper-level exit pressure (1,196 - 1,222 kPa) ratios of $\Delta P/P_w$ both fall above and below the solid line.

3.2 Peak Overpressure vs. Distance--Flattop Exit Pressure. To alert the reader to the type of pressure-vs.-time records exiting the shock tube, plots of the shock tube flattop wave and decaying wave are shown in Figure 4. Also shown in Figure 4 is a long-duration decaying wave as measured from the high explosives tests (Coulter, Bulmash, and Kingery 1988). It is not expected that a flattop pressure pulse will occur from accidental explosions in underground munition storage sites. But if there is an effect on outside peak overpressure or impulse because of the overpressure vs. time in the exit-pressure pulse, then it should become apparent from these two conditions.

The data using the 150-cm-long driver from three different exit pressure ranges (503 to 553 kPa), (917 to 1,317 kPa) and (1,824 to 1,953 kPa) are listed in Table 2. The same parameters are listed here as in Table 1 and the listed pressure data are plotted in Figure 5. It can be seen in Figure 5 that beyond a distance of 10 diameters the ratios of $\Delta P/P_w$ are all plotted above the solid line representing Equation 1 (Skjeltrojs, Jensen, and Rinuan 1977). This figure would imply that there is some influence or a relationship between the exit-pressure wave shape and the pressure measured along the zero line outside of the tunnel.

It should be noted that some high explosives tests have also shown a trend where most of the data points of $\Delta P/P_w$ vs. R/D_T fall above the solid line established from Equation 1 (Coulter, Bulmash, and Kingery 1988). The exit pressures from this test were decaying shock waves but were also long-duration (relative to ours) waves (see Figure 4). Thus, the data points might be expected to fall in between the short-duration rapid decay and the longer duration flattop wave. By way of comparison, data from Test 3 (Coulter, Bulmash, and Kingery 1988) are plotted in Figure 5, and the ratios fall above the solid line.

3.3 Impulse vs. Distance--Decaying Exit Pressure. The positive pressure impulse has usually been ignored in establishing the Q-D criteria. The scaling procedure for impulse is different than for peak overpressure. As the yield or mass of explosive is increased, the distance from the explosion at which you would expect a given peak overpressure is a function of the cube root of the mass. The peak overpressure is not scaled. When scaling impulse, one must remember that as the amount of explosive is increased the distance and impulse are both increased. The scaling relationships are well established for explosives detonated in the atmosphere without confinement.

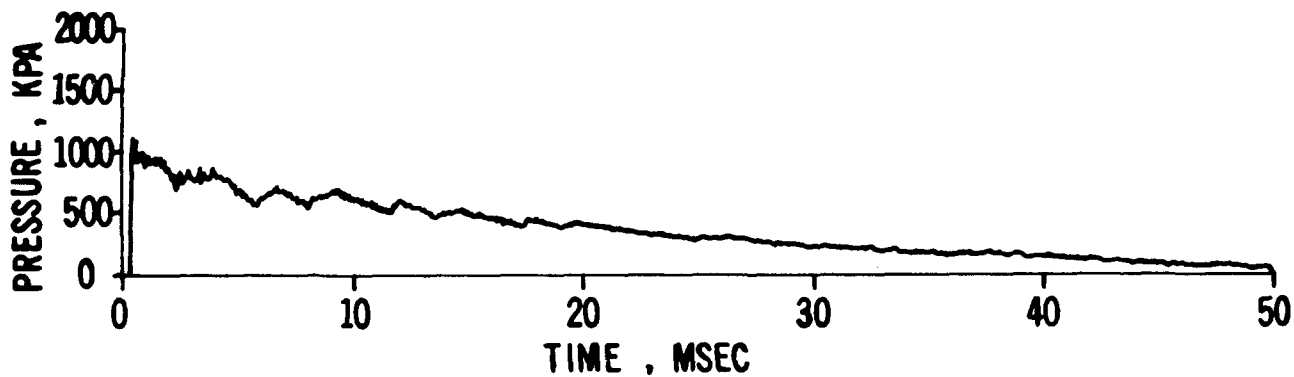
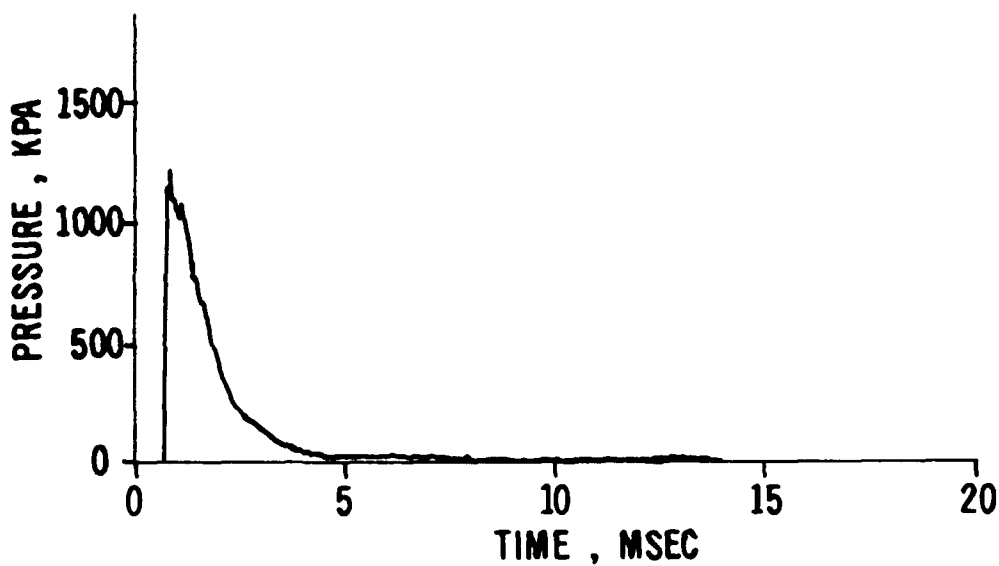
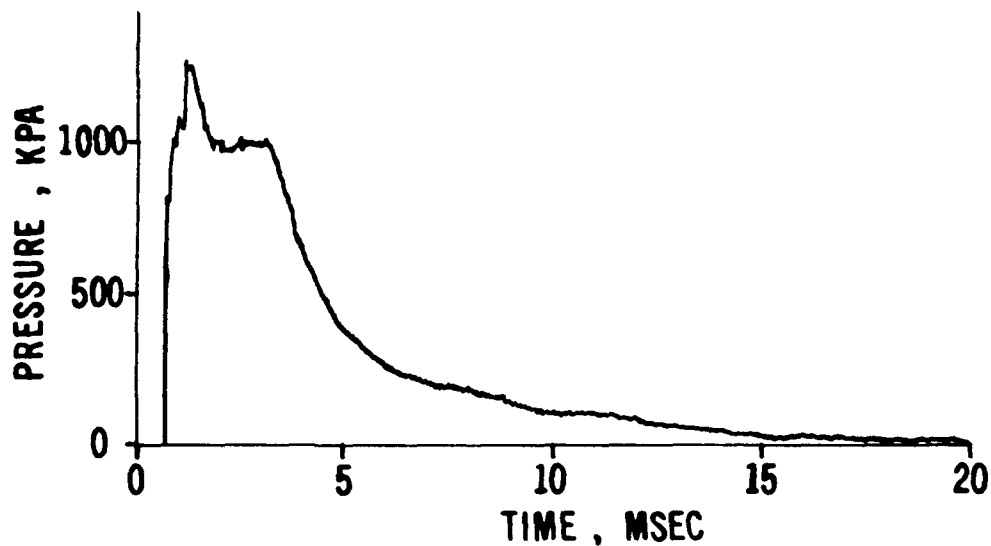


Figure 4. Tunnel-Exit Overpressure vs. Time for Shock Tube Flattop and Decaying Wave Forms and a High-Explosive, Test Model, Decaying Wave.

TABLE 2. Side-On Peak Pressure and Impulse Along the Zero-Degree Line--Long-Duration Flattop Exit Wave.

Test no.	Distance ratio, R/D_T	P_w , kPa	ΔP , kPa	Pressure		I_w , kPa -msec	I_s , kPa -msec	Impulse ratio, $\Delta I_s/I_w$
				ratio, $\Delta P/P_w$				
15	4.5	553	69.0	0.1250	1,462	36.20	0.0250	
14	4.5	514	86.3	0.1680	1,545	58.00	0.0380	
15	6.5	553	42.8	0.0770	1,462	15.00	0.0103	
14	6.5	514	53.2	0.1040	1,545	20.30	0.0130	
13	10.0	503	32.1	0.0640	1,298	16.60	0.0130	
13	15.0	503	36.5	0.0730	1,298	13.70	0.0110	
15	23.0	553	15.0	0.0270	1,462	10.30	0.0071	
14	23.0	514	12.6	0.0250	1,545	11.20	0.0073	
13	35.0	503	13.6	0.0270	1,298	2.92	0.0023	
13	54.0	503	5.0	0.0099	1,298	0.78	0.0006	
9	4.5	961	107.1	0.1110	3,382	40.00	0.0120	
14	4.5	1056	99.6	0.0940	5,370	36.50	0.0068	
9	6.5	961	73.6	0.0770	3,382	17.00	0.0050	
44	6.5	1056	99.2	0.0940	5,370	79.10	0.0150	
12	10.0	917	56.9	0.0580	3,460	26.80	0.0078	
12	15.0	917	40.3	0.0420	3,460	22.00	0.0064	
9	23.0	961	25.0	0.0260	3,382	12.30	0.0036	
44	23.0	1056	32.0	0.0300	5,370	23.40	0.0044	
12	35.0	917	16.3	0.0170	3,460	10.20	0.0029	
12	54.0	917	7.9	0.0082	3,460	2.40	0.0007	
10	6.5	1824	158.4	0.0870	9,879	124.8	0.0130	
10	10.0	1824	110.0	0.0603	9,879	37.5	0.0038	
11	15.0	1953	97.8	0.0500	11,008	31.6	0.0029	
11	23.0	1953	60.1	0.0310	11,008	47.3	0.0043	
10	35.0	1824	46.8	0.0260	9,879	38.3	0.0040	
11	54.0	1953	17.3	0.0110	11,008	8.8	0.0008	
11	100.0	1953	6.1	0.0031	11,008	4.0	0.0004	

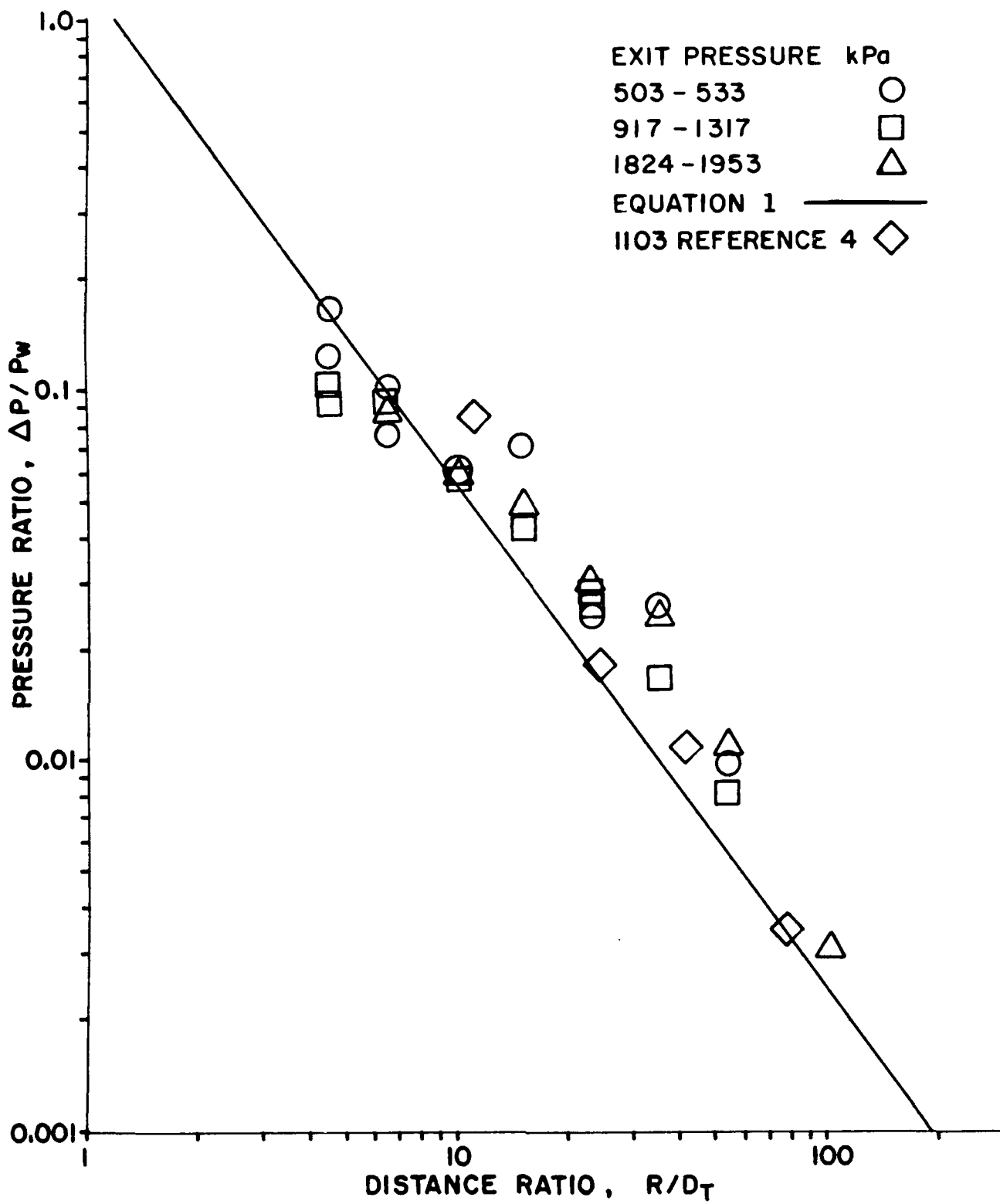


Figure 5. Pressure Ratio $\Delta P/P_w$ vs. Distance Ratio R/D_T for a Flattop and Long-Duration, Decaying Pressure Pulse.

In this report, we are dealing with a shock wave created from a compression chamber, then exiting into the atmosphere. The method for scaling the peak pressure and impulse propagating into the atmosphere as a function of the pressure or impulse at the end of the shock tube is quite complex. Efforts to establish methods for predicting this free-field impulse outside of shock tubes and gun barrels have been ongoing for many years. One of these methods uses the decay time of the energy efflux for the jet flow as a significant parameter for predicting free-field impulse (Fansler 1986). Equation 1 appears to be adequate for predicting ΔP for many decaying exit pressure-time conditions but did not fit the data from flattop shock waves.

The positive pressure impulses I_w from the short-duration decaying waves exiting the shock tube are listed in Table 2. Also listed in Table 2 are the impulse values I_s recorded at the selected distance along the zero line. The impulse ratios of I_s/I_w vs. distance ratio R/D_T are plotted in Figure 6. It appears from this plot that the magnitude of the exiting impulse I_w has some influence on the ratios at distances less than 10 tube diameters. That is, the larger the exit impulse, the smaller the ratio. At 10 diameters and beyond, the ratios follow a reasonable trend. The following equation,

$$I_s/I_w = 0.5 (R/D_T)^{-1.35}, \quad (2)$$

appears to fit the data reasonably well for R/D_T greater than 10.

The exponent -1.35 is the same as developed in Equation 1 for the pressure ratios.

If we assume that the impulse recorded at the end of the shock tube can be treated as a measure of energy, then it may be possible to establish a method of scaling that would show better correlation of results than Figure 6. From Table 2, the listed values of I_w are assumed a measure of energy, and cube-root scaling will be attempted (i.e., the values of R/D_T and I_s will be divided by $(I_w)^{1/3}$). These "scaled" values are presented in Table 3. Columns 3 and 6 of Table 3 are plotted in Figure 7. An equation, in the form of

$$I_s/(I_w)^{1/3} = 1.9 \{(R/D_T)/(I_w)^{1/3}\}^{-1.35}, \quad (3)$$

gives a reasonably good fit to the data presented in Figure 7 for $(R/D_T)/(I_w)^{1/3}$ greater than 1.0. There is still some scatter at scaled distances less than 1.0. It is quite possible that the vortex exiting the tube may have some effect on the duration of the pressure-vs.-time record and, therefore, the impulse, and this may not be a scaleable parameter close to the tunnel exit.

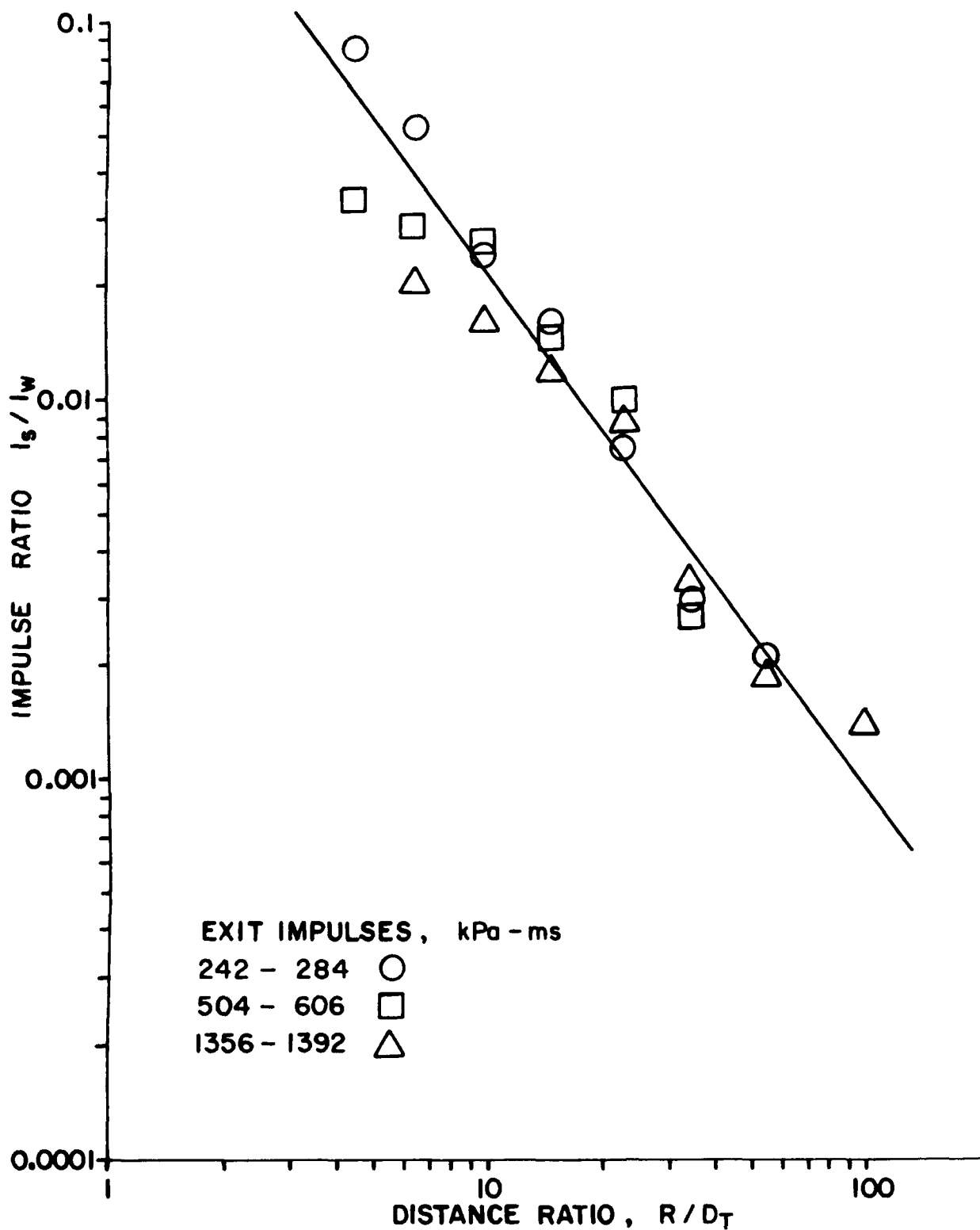


Figure 6. Impulse Ratio I_s/I_w vs. Distance Ratio R/D_T for a Short-Duration, Decaying Exit-Pressure Pulse.

TABLE 3. Side-On Scaled Impulse and Scaled Distance Ratio for Short-Duration, Decaying Exit Wave.

Test no.	Distance ratio, R/D_T	Scaled distance ratio, $(R/D_T)/(I_w)^{1/3}$	Impulse I_w , kPa -ms	Impulse I_s , kPa -ms	Scaled impulse, $I_s/(I_w)^{1/3}$
16	4.5	0.69	284	24.8	3.77
16	6.5	0.99	284	14.7	2.24
16	10.0	1.52	284	6.8	1.04
17	15.0	2.41	242	4.0	0.64
16	23.0	3.50	284	1.9	0.29
17	35.0	5.62	242	0.7	0.11
17	54.0	8.67	242	0.5	0.08
8	4.5	0.53	606	20.8	2.46
8	6.5	0.77	606	17.5	2.07
19	10.0	1.26	504	13.1	1.65
19	15.0	1.89	504	7.4	0.93
8	23.0	2.72	606	6.1	0.72
19	35.0	4.40	504	1.4	0.18
21	6.5	0.59	1,356	27.7	2.50
21	10.0	0.90	1,356	21.8	1.97
20	15.0	1.34	1,392	16.3	1.46
21	23.0	2.08	1,356	11.9	1.08
20	35.0	3.14	1,392	4.6	0.41
20	54.0	4.84	1,392	2.6	0.23
20	100.0	8.96	1,392	1.2	0.11

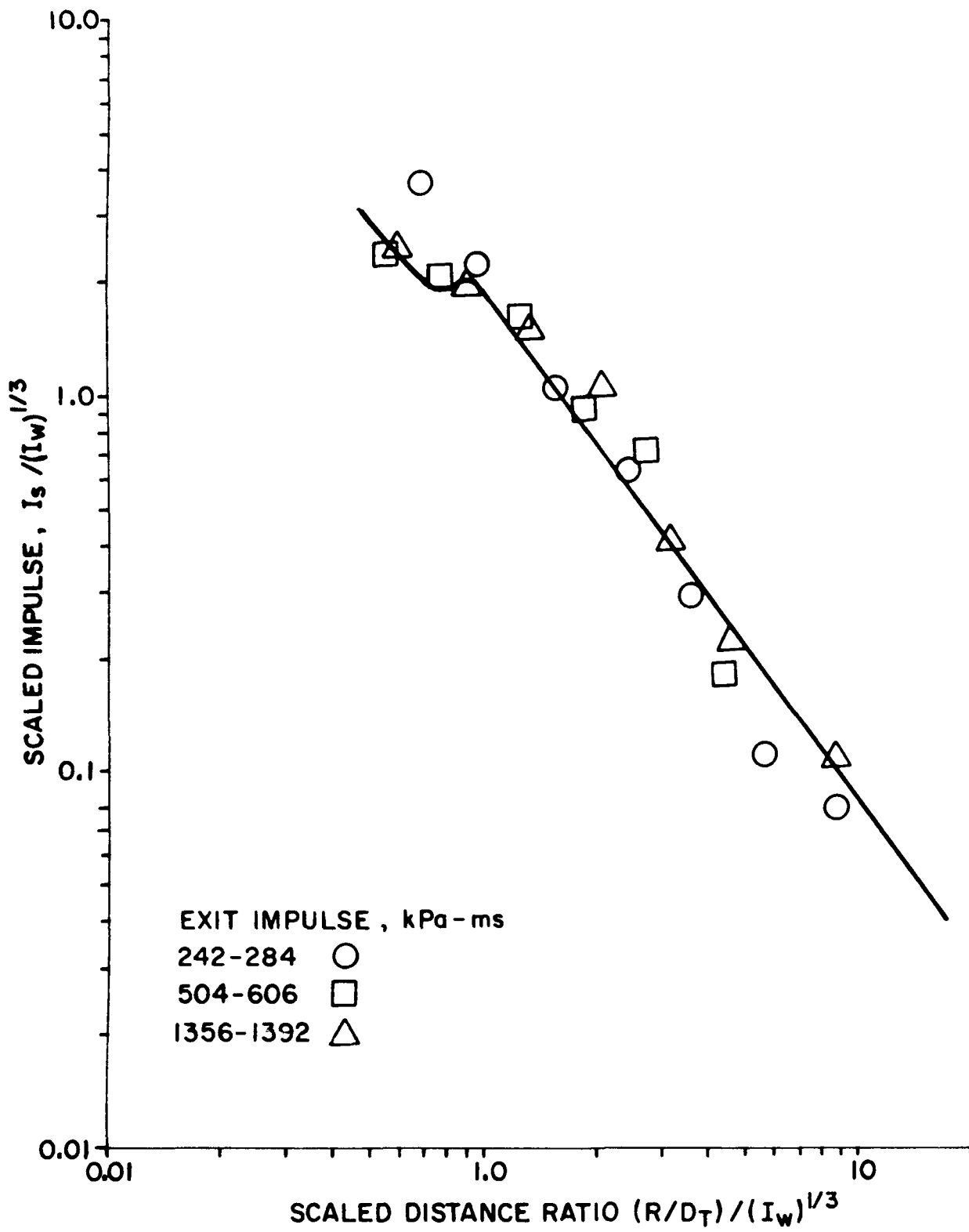


Figure 7. Scaled Impulse vs. Scaled Distance Ratio for a Short-Duration, Decaying Exit-Pressure Pulse.

Moving $I_w^{1/3}$ to the right side of Equation 3, we find we can calculate I_s from Equation 4. If we know I_w , then

$$I_s = 1.9 (R/D_T)^{-1.35} (I_w)^{0.783}. \quad (4)$$

Equations 3 and 4 are good only for short-duration decaying exit pressures at $(R/D_T)/(I_w)^{1/3}$ greater than 1.0.

3.4 Impulse vs. Distance--Flat-top Exit Pressure. The ratios of I_s/I_w vs. R/D_T listed in Table 2 were plotted on log-log paper, but there was no correlation between the different ranges of exit impulses; in order to determine the trend of impulse vs. distance, the individual values of I_s vs. R/D_T were plotted in Figure 8.

The measured impulses I_s were normalized to an average I_w for the three different exit impulse levels. That is, the lower level I_s values plotted in Figure 8 are $1,420/I_w \times I_s = I_{sn}$, when I_{sn} is the normalized value. The mid-level values were normalized to an I_w of 4,000 kPa-ms, and the high-level values were normalized to an I_w of 10,500 kPa-ms. These three normalized curves are plotted in Figure 8. Here it can be seen that there is an initial decay, then a rise in impulse, followed by a second decay in impulse vs. distance.

The same cube-root scaling techniques used to establish the curve presented in Figure 7 for the decaying exit-pressure impulse has been applied to the "flat-top" exit-pressure impulses in Table 4. The values of $(R/D_T)/(I_w)^{1/3}$ vs. $I_s/(I_w)^{1/3}$ from Table 4 have been plotted in Figure 9. While there is some scatter of data points, the trend shown in Figure 8 is still evident in Figure 9. No attempt has been made to develop an equation for the curve in Figure 9, but if I_w is known, then the side-on impulse can be determined for different distance ratios of R/D_T .

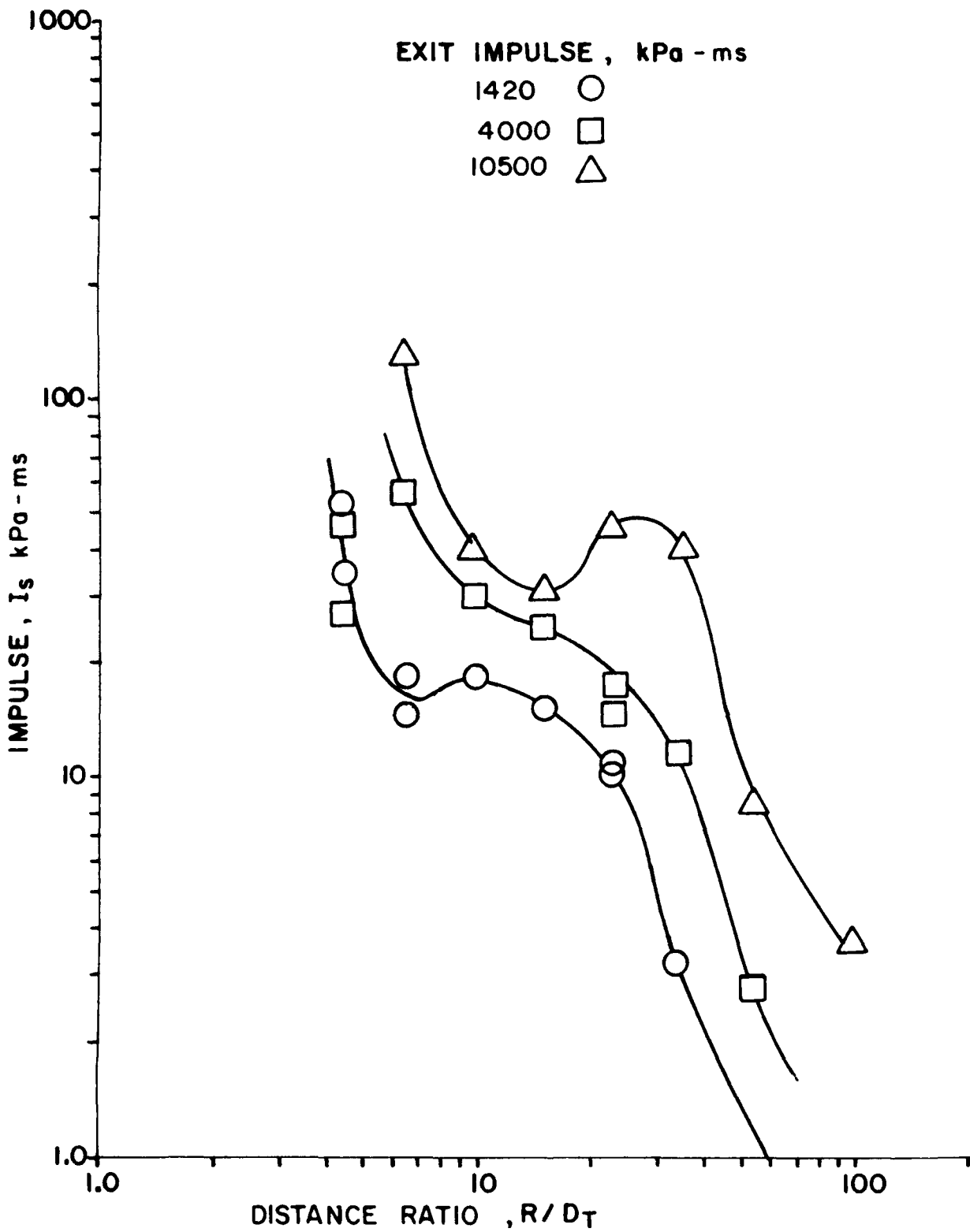


Figure 8. Measured Impulse I_s vs. Distance Ratio R/D_T for Three Flattop Exit-Impulse Ranges.

TABLE 4. Side-On Scaled Impulse and Scaled Distance Ratio for a Flattop Exit Wave.

Test no.	Distance ratio, R/D_T	Scaled distance ratio, $(R/D_T)/(I_w)^{1/3}$	Impulse I_w , kPa -ms	Impulse I_s , kPa -ms	Scaled impulse, $I_s/(I_w)^{1/3}$
15	4.5	0.40	1,462	36.2	3.19
14	4.5	0.39	1,545	58.0	5.02
15	6.5	0.57	1,462	15.0	1.32
14	6.5	0.56	1,545	20.3	1.76
13	10.0	0.92	1,298	15.6	1.52
13	15.0	1.38	1,298	13.7	1.26
15	23.0	2.03	1,462	10.3	0.91
14	23.0	1.99	1,462	11.2	0.97
13	35.0	3.21	1,298	2.9	0.27
13	54.0	4.95	1,298	0.8	0.07
9	4.5	0.30	3,382	40.0	2.67
44	4.5	0.26	5,370	36.5	2.07
9	6.5	0.43	3,382	17.0	1.13
44	6.5	0.37	5,370	79.1	4.49
12	10.0	0.66	3,460	26.8	1.77
12	15.0	0.99	3,460	22.0	1.46
9	23.0	1.53	3,382	13.3	0.82
44	23.0	1.31	5,370	23.4	1.33
12	35.0	2.31	3,460	16.2	0.67
12	54.0	3.57	3,460	2.4	0.16
10	6.5	0.30	9,879	124.8	5.82
10	10.0	0.47	9,879	37.5	1.75
11	15.0	0.67	11,008	31.6	1.42
11	23.0	1.03	11,008	47.3	2.13
10	35.0	1.63	9,879	38.3	1.78
11	54.0	2.43	11,008	8.8	0.40
11	100.0	4.50	11,008	4.0	0.18

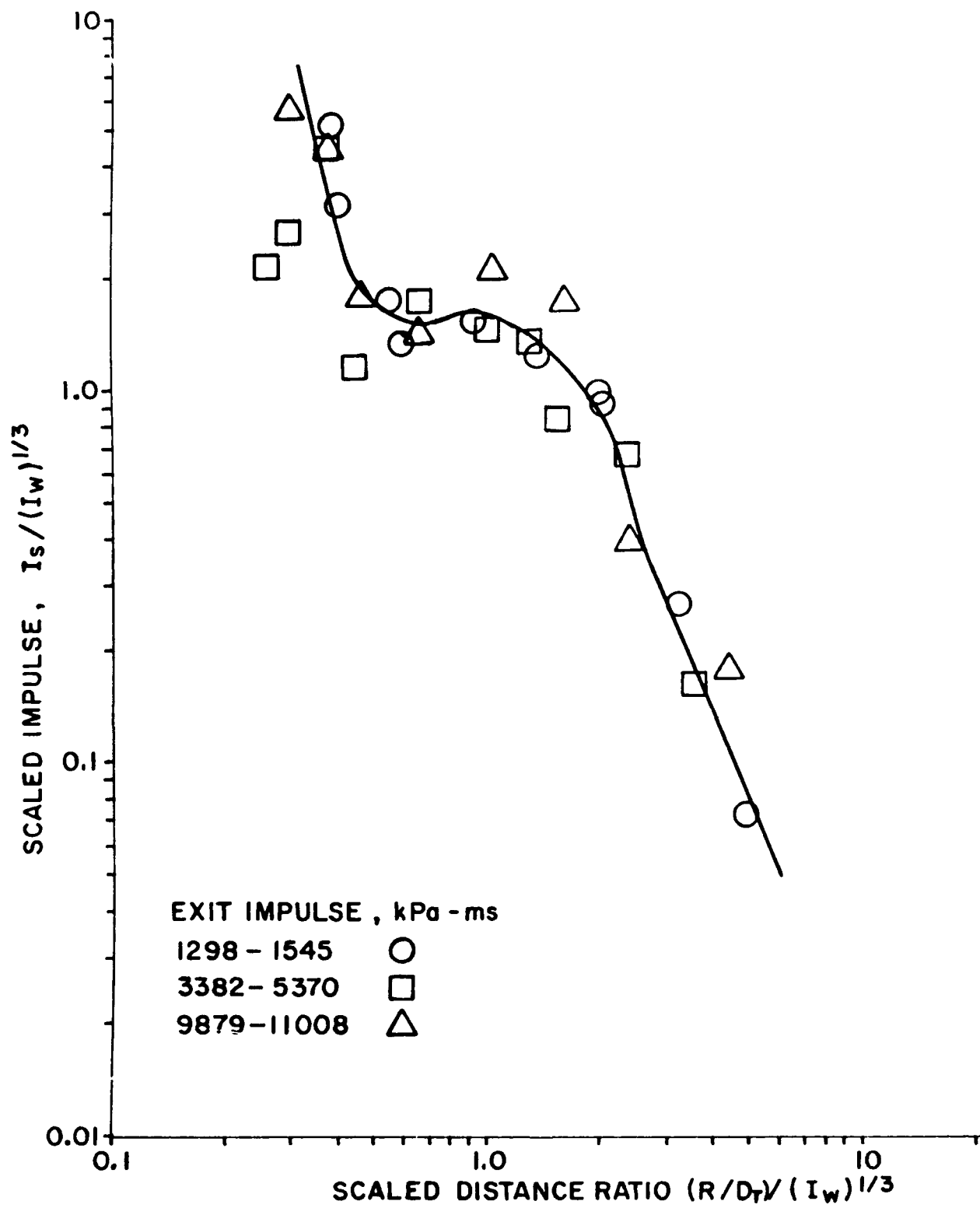


Figure 9. Scaled Impulse vs. Scaled Distance Ratio for Flat-top, Exit-Pressure Pulses.

4. CONCLUSIONS

In the previous sections we have looked at two quite different blast waves simulating an explosion in a storage magazine tunnel. A 2.54-cm-diameter shock tube was used to simulate the blast waves. The effects in the "field" overpressure, due to an exiting, short-duration blast wave and that due to a flattop, long-duration blast wave, were considered to determine if the durations of the waves had the same relationship and influence on the blast measurements.

Principally, it was found that the short-duration exiting wave's pressures were adequately handled by a standard equation developed by the Norwegians (Skjeltrojs, Jensen, and Rinuan 1977). The impulse was better predicted and correlated when impulse and nondimensional distance R/D_T were both scaled by $I_w^{1/3}$, the exit impulse to the 1/3 power. The intent here was to account for the energy exiting the tube and is analogous to the 1/3-powers law for free-field explosions.

On the other hand, for the long-duration, flattop exiting wave, subtle differences are noted, when the overpressure data are plotted following the standard procedure P/P_w vs. R/D_T . Such a result suggests that the wave duration does have an influence on the peak overpressure field measurements. Additionally, using the $I_w^{1/3}$ scaling on the long-duration impulse data produces a rather good correlation of the data (Figure 9) as was seen for the short-duration data. Thus, whatever the wave shape or blast-wave duration exiting, it seems possible, with a measurement of the exit impulse, to predict with greater assurance the resulting impulse outside.

INTENTIONALLY LEFT BLANK.

5. REFERENCES

1. U.S. Department of Defense Explosives Safety Board. Ammunition and Explosives Safety Standards. DoD 6055.9-STD, Alexandria, VA, July 1984.
2. Coulter, G.A., G. Bulmash, and C.N. Kingery. "Simulation Techniques for Prediction of Blast from Underground Munition Storage Sites." BRL-MR-3659, U.S. Army Ballistic Research Laboratory, Aberdeen Proving Ground, MD, April 1988.
3. Fansler, K.S. "Dependence of Free-Field Impulse on the Decay Time of Energy Efflux for a Jet Flow." BRL-MR-3516, U.S. Army Ballistic Research Laboratory, Aberdeen Proving Ground, MD, May 1986.
4. Kingery, C.N. "Survey of Airblast Data Related to Underground Storage Sites." BRL-MR-3769, U.S. Army Ballistic Research Laboratory, Aberdeen Proving Ground, MD, June 1989.
5. Skjeltrojs, A.T., A. Jensen, and A. Rinuan. "Blast Propagation Outside a Typical Ammunition Storage Site." Paper presented at the proceedings of the Fifth International Symposium on Military Applications of Blast Simulation, Stockholm, Sweden, May 22-26, 1977.
6. Zardas, S.J. "Free-Field Stagnation Pressure and Impulse from H.E. Detonation in a Model Underground Munitions Storage Facility." U.S. Army Ballistic Research Laboratory, Aberdeen Proving Ground, MD, to be published.

INTENTIONALLY LEFT BLANK.

APPENDIX:
DATA FROM DETONATIONS OF HIGH
EXPLOSIVE IN MUNITION STORAGE MODELS

INTENTIONALLY LEFT BLANK.

INTRODUCTION

The data from high explosives detonations presented in this appendix were taken from two sources, which are References 2 and 6 (Coulter, Bulmash, and Kingery 1988; Zardas, to be published). The methods used in acquiring the results and analysis of results are fully documented and will not be repeated here. The work presented in this report is from a small-diameter (2.54 cm) shock tube where two different driver lengths were used to develop different exit-pressure pulses, a decaying shock wave and a flattop shock wave.

The data from the two references are of interest because they are based on a long-duration, decaying shock wave, which more nearly represents the type of pressure pulse that would exit an underground storage site in the event of an accidental explosion.

PEAK OVERPRESSURE OUTSIDE THE TUNNEL EXIT

The peak overpressures recorded outside of the tunnel exit vs. distance along the zero-degree line are listed in Table A-1 (Coulter, Bulmash, and Kingery 1988). The values of peak side-on overpressure are plotted in Figure A-1 as pressure ratio $\Delta P/P_w$ vs. distance ratio R/D_T . Here, as in Figure 5, the values of $\Delta P/P_w$ are above the standard curve at distance ratios R/D_T greater than 1. There appears to be a correlation between the increase in the duration or impulse in the exit pressure and an increase in the pressure ratio $\Delta P/P_w$.

A similar series of tests as described in Coulter, Bulmash, and Kingery (1988) was also conducted and described in Zardas (to be published). The data from Zardas are listed in Table A-2. The pressure-distance values are plotted Figure A-2 as pressure ratio $\Delta P/P_w$ vs. distance ratio R/D_T . Here again, the plotted pressure ratios are higher than the standard curve and also appear to have a greater negative slope. An equation was developed which fits both sets of data.

$$\frac{\Delta P}{P_w} = 3.6 \left(\frac{R}{D_T} \right)^{-1.58} \quad (1)$$

This equation should not be used at R/D_T less than 7 or greater than 100.

TABLE A-1. Peak Overpressure and Impulse Data.

Test no.	Distance ratio, R/D_T	Side-on pressure, ΔP kPa	Pressure ratio, $\Delta P/P_w$	Side-on impulse, I_s kPa-ms	Scaled impulse ratio, $I_s/I_w^{1/3}$	Scaled distance ratio, $(R/D_T)/(I_w)^{1/3}$
Test 1						
0-1	4.58	90.0	0.190	140.0	7.70	0.252
0-2	9.95	35.0	0.074	46.0	2.52	0.548
0-3	17.00	31.0	0.065	27.5	1.51	0.934
0-4	31.90	10.0	0.021	8.7	.48	1.760
						$P_w = 475$ kPa $I_w = 6,000$ kPa-ms $I_w^{1/3} = 18.2$
Test 2						
0-1	6.91	123.0	0.160	72.0	3.50	0.335
0-2	15.05	33.0	0.043	35.0	1.70	0.731
0-3	25.73	15.9	0.020	16.0	0.77	1.250
0-4	48.16	4.9	0.006	6.0	0.29	2.340
						$P_w = 765$ kPa $I_w = 8,800$ kPa-ms $I_w^{1/3} = 20.6$
Test 3						
0-1	11.0	98.0	0.089	64.0	2.37	0.407
0-2	23.92	20.0	0.018	35.0	1.30	0.896
0-3	41.01	11.7	0.001	18.0	0.67	1.560
0-4	76.70	3.8	0.0034			
						$P_w = 1,103$ kPa $I_w = 20,000$ kPa-ms $I_w^{1/3} = 27.0$
Test 4						
0-1	18.30	47.6	0.031	112.0	3.34	0.547
0-2	39.80	15.2	0.010	43.5	1.30	1.190
0-3	68.50	13.9	0.009	20.0	0.60	2.050
0-4	128.10	5.0	0.003	8.0	0.24	3.830
						$P_w = 1,551$ kPa $I_w = 37,500$ kPa-ms $I_w^{1/3} = 33.5$

Source: Coulter, Bulmash, and Kingery, 1988.

Note: $D_T = 0.1016$ m.

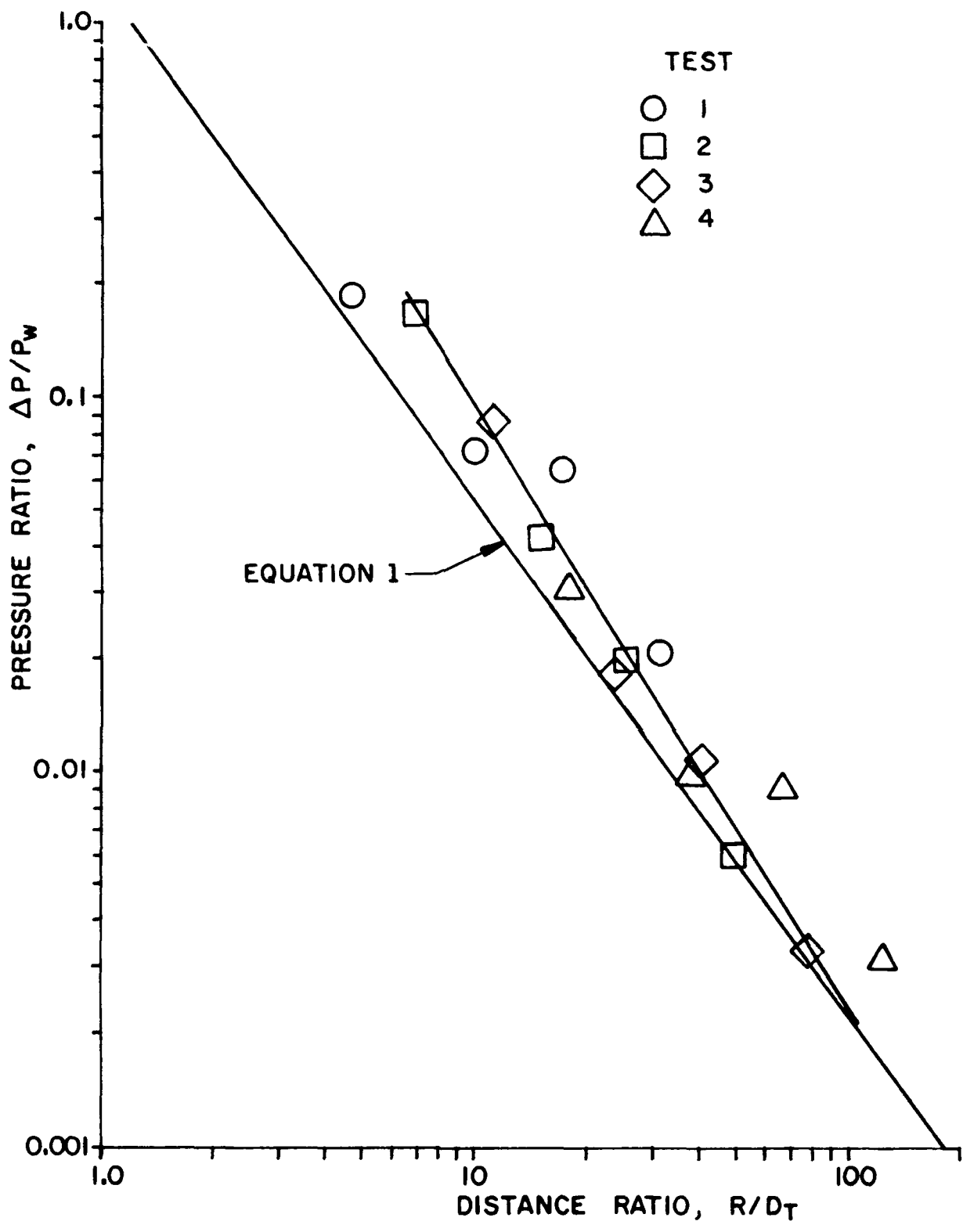


Figure A-1. Pressure Ratio $\Delta P/P_w$ vs. Distance Ratio R/D_T (from Reference 2).

TABLE A-2. Peak Overpressure and Impulse Data.

Test no.	Distance ratio, R/D_T	Side-on pressure, ΔP kPa	Pressure ratio, $\Delta P/P_w$	Side-on impulse, I_s kPa-ms	Scaled impulse ratio, $I_s/I_w^{1/3}$	Scaled distance ratio, $(R/D_T)/(I_w)^{1/3}$
Test 1						
0-1	9.84	58	.089	38.1	1.94	0.50
0-2	15.1	33	.051	39.2	2.00	0.77
0-3	25.7	11	.017	17.3	0.88	1.31
0-4	48.1	4.30	.007	5.6	0.29	2.45
Test 2						
0-1	9.84	100	.133	44.1	2.05	0.46
0-2	15.1	33	.044	40.2	1.87	0.70
0-3	25.7	12	.016	24.3	1.13	1.19
0-4	48.1	4.3	.006	4.7	0.22	2.24
Test 3						
0-1	11.8	84	.093	57.8	2.27	0.46
0-2	23.9	19/24	.021	35.9	1.41	0.94
0-3	41.0	9.7	.011	19.1	0.75	1.61
0-4	76.8	3.3	.004	7.7	0.30	3.01
Test 4						
0-1	11.8	75	.094	75.1	2.83	0.46
0-2	23.9	19/31	.024	74.8	2.82	0.90
0-3	41.0	10/15	.013	67.2	2.54	1.55
0-4	76.8	3.9	.005	15.3	0.58	2.90
Test 5						
0-1	11.8	83	.072	85.4	3.23	0.45
0-2	23.9	27/40	.024	78.2	2.96	0.91
0-3	41.0	10/11	.009	77.9	2.95	1.55
0-4	76.8	4.5	.004	16.8	0.64	2.91

$P_w = 650$
 $I_w = 7,573$ kPa-ms
 $I_w^{1/3} = 19.64$

$P_w = 750$
 $I_w = 9,984$ kPa-ms
 $I_w^{1/3} = 21.5$

$P_w = 900$
 $I_w = 16,635$ kPa-ms
 $I_w^{1/3} = 25.5$

$P_w = 800$
 $I_w = 18,539$ kPa-ms
 $I_w^{1/3} = 26.5$

$P_w = 1,150$
 $I_w = 18,492$ kPa-ms
 $I_w^{1/3} = 26.4$

Source: Zardas, to be published.

Note: $D_T = 0.1016$ m; tests 4 and 5 were not used in the impulse comparisons in Figure A-3 because plywood replaced the sand base.

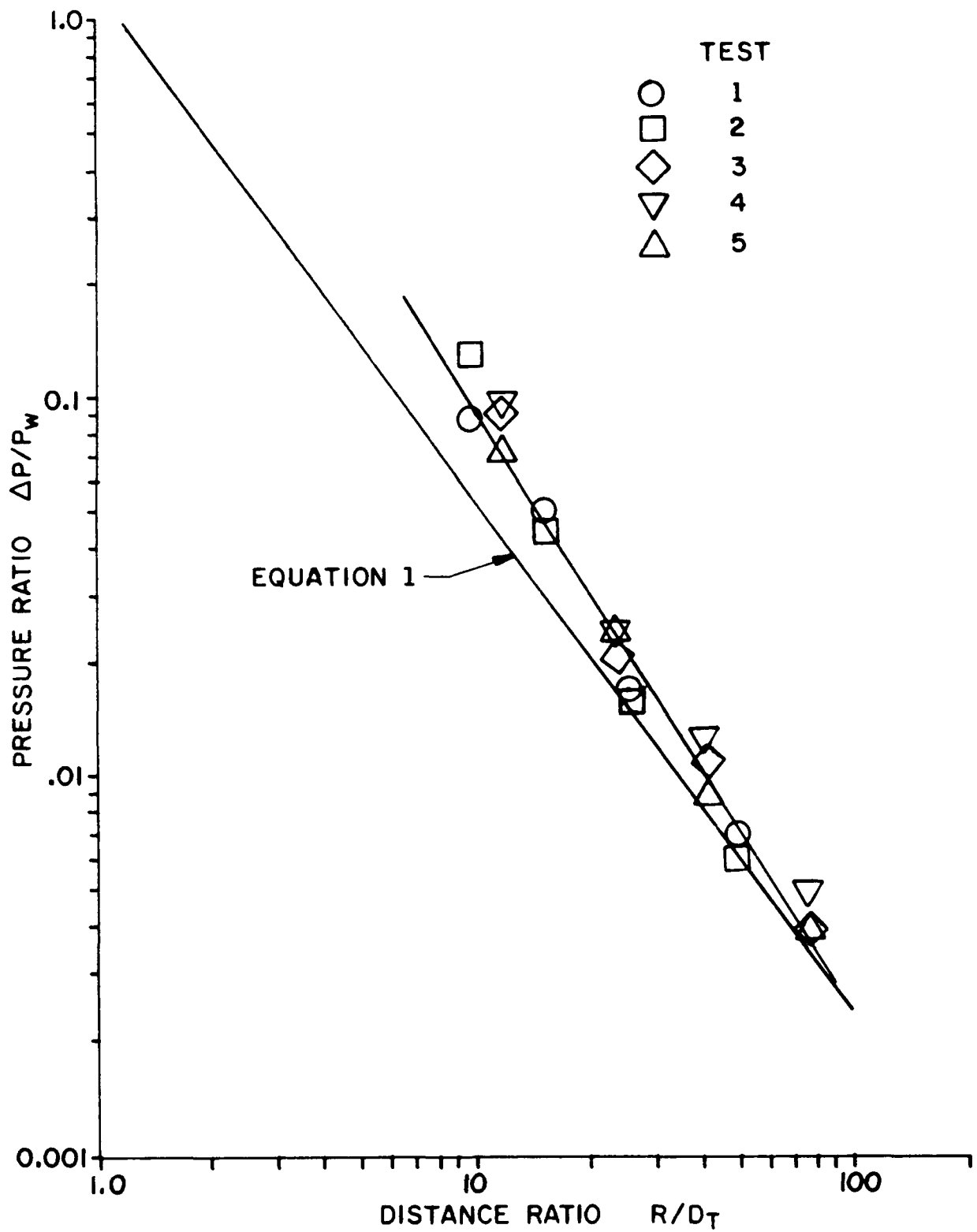


Figure A-2. Pressure Ratio $\Delta P/P_w$ vs. Distance Ratio R/D_T (from Reference 6).

PEAK OVERPRESSURE IMPULSE OUTSIDE THE TUNNEL EXIT

The overpressure impulses from References 2 and 6, both side-on (I_s) and exit (I_w), have been treated as described in Section 3.3 of the main report. The measured values, scaled values, and scaled ratios are listed in Tables A-1 and A-2. The impulse data from Tables A-1 and A-2 are plotted in Figure A-3. It can be seen in Figure A-3 that, at scaled distance values less than 0.7, there is a trend similar to that noted from the shock tube data in Figure 9. At scaled distance ratios greater than 0.7, a simple equation,

$$\frac{\Delta I_s}{(\Delta I_w)^{1/3}} = 1.2 \left(\frac{R/D_T}{I_w^{1/3}} \right)^{-1.35} \quad (2)$$

gives a reasonable fit to the plotted data beyond $(R/D_T)/(I_w)^{1/3}$ equal to 0.7.

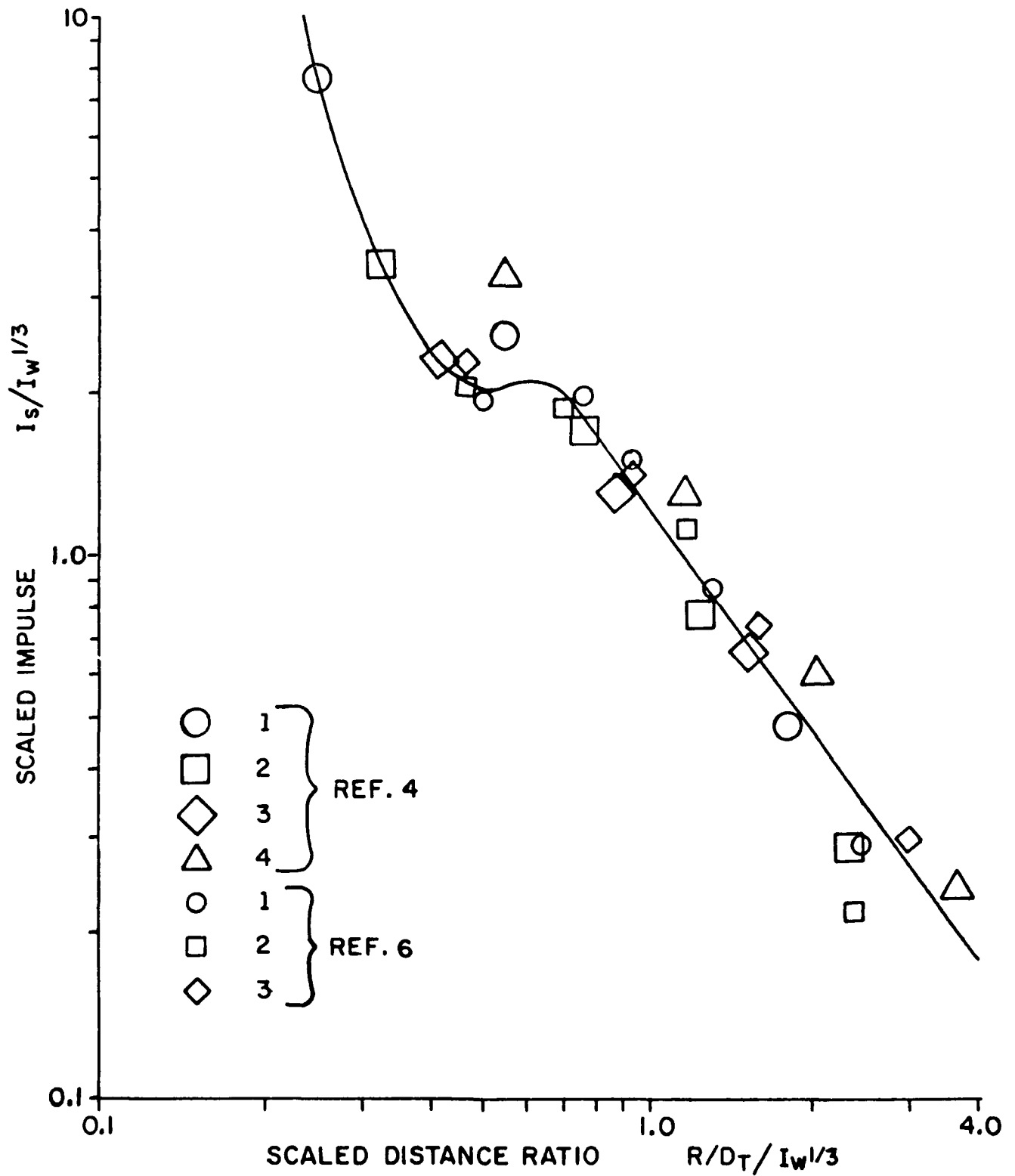


Figure A-3. Scaled Impulse $I_s/I_w^{1/3}$ vs. Scaled Distance Ratio $(R/D_T)/(I_w)^{1/3}$
 (from References 2 and 6).

CONCLUSIONS

There are two conclusions based on the munition storage site model results. First the long-duration, decaying shock wave does have an effect on the peak overpressure measured at selected distances in front of the tunnel. The pressure ratio values are higher at given distance ratio values than the standard curve (Equation 1 in the text), and the negative slope is greater (see Equation 1).

A second conclusion based on the long-duration decaying wave is that the scaled values for the impulse ratio are lower at similar scaled distance ratios than the short-duration results in Figure 7. There is a similarity in the data presented in Figure A-3 for the long-duration decaying wave and that presented in Figure 9 for the long-duration, flattop shock wave. Based on the results measured from the shock tube and from the high-explosive test using a scaled model, it can be stated that the shock wave parameters exiting the tube or tunnel have an influence on the blast parameters measured outside of the tube.

<u>No of Copies</u>	<u>Organization</u>	<u>No of Copies</u>	<u>Organization</u>
1	Office of the Secretary of Defense OUSD(A) Director, Live Fire Testing ATTN: James F. O'Bryon Washington, DC 20301-3110	1	Director US Army Aviation Research and Technology Activity ATTN: SAVRT-R (Library) M/S 219-3 Ames Research Center Moffett Field, CA 94035-1000
2	Administrator Defense Technical Info Center ATTN: DTIC-DDA Cameron Station Alexandria, VA 22304-6145	1	Commander US Army Missile Command ATTN: AMSMI-RD-CS-R (DOC) Redstone Arsenal, AL 35898-5010
1	HQDA (SARD-TR) WASH DC 20310-0001	1	Commander US Army Tank-Automotive Command ATTN: AMSTA-TSL (Technical Library) Warren, MI 48397-5000
1	Commander US Army Materiel Command ATTN: AMCDRA-ST 5001 Eisenhower Avenue Alexandria, VA 22333-0001	1	Director US Army TRADOC Analysis Command ATTN: ATAA-SL White Sands Missile Range, NM 88002-5502
1	Commander US Army Laboratory Command ATTN: AMSLC-DL Adelphi, MD 20783-1145	(Class. only) 1	Commandant US Army Infantry School ATTN: ATSH-CD (Security Mgr.) Fort Benning, GA 31905-5660
2	Commander US Army, ARDEC ATTN: SMCAR-IMI-I Picatinny Arsenal, NJ 07806-5000	(Unclass. only) 1	Commandant US Army Infantry School ATTN: ATSH-CD-CSO-OR Fort Benning, GA 31905-5660
2	Commander US Army, ARDEC ATTN: SMCAR-TDC Picatinny Arsenal, NJ 07806-5000	1	Air Force Armament Laboratory ATTN: AFATL/DLODL Eglin AFB, FL 32542-5000
1	Director Benet Weapons Laboratory US Army, ARDEC ATTN: SMCAR-CCB-TL Watervliet, NY 12189-4050		<u>Aberdeen Proving Ground</u>
1	Commander US Army Armament, Munitions and Chemical Command ATTN: SMCAR-ESP-L Rock Island, IL 61299-5000	2	Dir, USAMSAA ATTN: AMXSY-D AMXSY-MP, H. Cohen
1	Commander US Army Aviation Systems Command ATTN: AMSAV-DACL 4300 Goodfellow Blvd. St. Louis, MO 63120-1798	1	Cdr, USATECOM ATTN: AMSTE-TD
		3	Cdr, CRDEC, AMCCOM ATTN: SMCCR-RSP-A SMCCR-MU SMCCR-MSI
		1	Dir, VLAMO ATTN: AMSLC-VL-D

<u>No. of Copies</u>	<u>Organization</u>	<u>No. of Copies</u>	<u>Organization</u>
30	Chairman DOD Explosives Safety Board ATTN: JDDESB Hoffman Bldg 1, Room 856-C 2461 Eisenhower Avenue Alexandria, VA 22331-0600	4	Director Defense Nuclear Agency ATTN: SPTD (Mr. Kennedy) DDST(E) (Dr. Sevin) OALG (Mr. Jeffers) LEEE (Mr. Eddy) Washington, DC 20305
1	OSD, ADUSDRE (R/AT,ET) ATTN: Mr. J. Persh Washington, DC 20301-3110	1	Information & Analysis Ctr-DNA Kaman Tempo ATTN: DASIAC P.O. Drawer QQ Santa Barbara, CA 93102
1	Under Secretary of Defense for Research & Engineering Department of Defense Washington, DC 20301	6	HQDA (DAEN-ECE-T/Mr. Wright) (DAEN-MCC-D/Mr. Foley) (DAEN-RDL/Mr. Simonini) (DAEN-RDZ-A/Dr. Choromokos) (DALO-SMA/COL Paris) (DAPE-HRS) WASH DC 20310-0001
1	Director of Defense Research & Engineering Washington, DC 20301	1	Commander US Army Materiel Command ATTN: AMCSF 5001 Eisenhower Avenue Alexandria, VA 22333-0001
1	Assistant Secretary of Defense (Atomic Energy) ATTN: Document Control Washington, DC 20301	1	Director AMC Field Safety Activity ATTN: AMXOS-OES Charlestown, IN 47111-9669
1	Assistant Secretary of Defense (MRA&L) ATTN: EO&SP Washington, DC 20301	1	Director AMC ITC ATTN: Dr. Chiang Red River Depot Texarkana, TX 75501
1	Director Defense Advanced Research Projects Agency 1400 Wilson Boulevard Arlington, VA 22209-2308	1	Commander USA Laboratory Command ATTN: AMSLC-AS-SE (R. Oden) 2800 Powder Mill Road Adelphi, MD 20783-1145
1	Director Defense Intelligence Agency ATTN: DT-1B (Dr. Vorona) Washington, DC 20301	1	Director U.S. Army Materials Technology Laboratory ATTN: SLCMT-ATL Watertown, MA 02172-0001
2	Chairman Joint Chiefs of Staff ATTN: J-3 (Operations) J-5 (P&P/R&D Div) Washington, DC 20301	1	Commander USA Harry Diamond Laboratories ATTN: SLCHD-TI 2800 Powder Mill Road Adelphi, MD 20783-1197
3	Director Institute for Defense Analyses ATTN: Dr. H. Menkes Dr. J. Bengston Tech Info Ofc 1801 Beauregard Street Alexandria, VA 22311		

<u>No. of Copies</u>	<u>Organization</u>
1	Commander USA Natick R&D Engineering Center ATTN: AMDNA-D (Dr. Seiling) Natick, MA 01760
2	Commander USA Armament Materiel Readiness Command ATTN: Joint Army/Navy/AF Conven Ammo Prof Coord GP/EI (Jordan) Rock Island, IL 61299
1	Commander USA Armament Command ATTN: AMSAR-SA Rock Island Arsenal Rock Island, IL 61201
1	Commander US Army Armament, Munitions and Chemical Command ATTN: AMSMC-IMP-L Rock Island, IL 61299-7300
1	Commander USA Armament Research, Development & Engineering Center ATTN: SMCAR-LCM-SPC Picatinny Arsenal, NJ 07806-5000
2	Commander USA Ballistic Missile Defense Systems Command ATTN: M. Whitfield, ATC J. Veeneman P.O. Box 1500 Huntsville, AL 35807-3801
1	Director Missile & Space Intelligence Center ATTN: AIAMS-YDL Redstone Arsenal, AL 35898-5500
1	Director USA TRADOC Analysis Center ATTN: ATOR-TSL White Sands Missile Range, NM 88002-5502
1	Commandant USA Engineer School ATTN: ATSE-CD Fort Leonard Wood, MO 65473-6620

<u>No. of Copies</u>	<u>Organization</u>
1	Commander USA Belvoir R&D Center ATTN: STRBE-NN Fort Belvoir, VA 22060-5606
1	Commander USA Engineer Division-Europe ATTN: EUDED (Dr. Crowson) APO, NY 09757
1	Division Engineer USA Engineer Division Fort Belvoir, VA 22060
1	Corps of Engineers-HSV Division ATTN: HNDDE (Mr. Char) P.O. Box 1600 Huntsville, AL 35807
1	Director USA Engineer Waterways Experimental Station ATTN: WESNB (K. Davis) P.O. Box 631 Vicksburg, MS 39180-0631
1	Commander USA Construction Engineering Research Laboratory P.O. Box 4005 Champaign, IL 61820
1	Commander USA Foreign Science & Technology Center ATTN: Rsch & Data Br Federal Office building 220 7th Street, NE Charlottesville, VA 22901
1	Commander USA Rock Island Arsenal Rock Island, IL 61299
1	Commander Indiana Army Ammunition Plant Charlestown, IN 47111
1	Commander Joliet Army Ammunition Plant Joliet, IL 60436
1	Commander Kansas Army Ammunition Plant Parsons, KS 67357
1	Commander Lone Star Army Ammunition Plant Texarkana, TX 75502

<u>No. of Copies</u>	<u>Organization</u>
1	Commander Longhorn Army Ammunition Plant Marshall, TX 75671
1	Commander Milan Army Ammunition Plant Milan, TN 38358
1	Commander Radford Army Ammunition Plant Radford, VA 24141
1	Commander Ravenna Army Ammunition Plant Ravenna, OH 44266
1	Commander Pine Bluff Arsenal Pine Bluff, AR 71601
1	Commander USA Aviation Systems Command ATTN: AMSAV-ES 4300 Goodfellow Boulevard St. Louis, MO 63120-1798
1	Commander USA Research Office P.O. Box 12211 Research Triangle Park, NC 27709-2211
1	Director Lewis Research Center ATTN: Mail Stop 77-5 21000 Brookpark Road Cleveland, OH 44135
1	Commander USA Communications Electronics Command ATTN: AMSEL-IM-L (Rpt Sec, B2700) Fort Monmouth, NJ 07703-5001
1	Commander US Army Missile Command ATTN: AMSMI-RR Redstone Arsenal, AL 35898-5249
1	Assistant Secretary of the Navy Research & Development Department of the Navy Washington, DC 20350

<u>No. of Copies</u>	<u>Organization</u>
3	Chief of Naval Operations ATTN: OP-411 (C. Ferraro) OP-41B CPT Wernsman Washington, DC 20350
2	Commander Naval Sea Systems Command ATTN: SEA-06H (Van Slyke) SEA-0333 Washington, DC 20362
4	Commander Naval Surface Warfare Center ATTN: Dr. Schindel Dr. Victor Dawson R15 (Swisdak/Smith) Silver Spring, MD 20902-5000
1	Commander Naval Weapons Center ATTN: Code 62C2 (Osterman) China Lake, CA 93555-6001
1	Commander Naval Research Lab ATTN: Code 2027 Washington, DC 20375
1	Commander Naval Weapons Evaluation Facility ATTN: Document Control Kirtland AFB Albuquerque, NM 87117
1	Officer-In-Charge Naval EOD Facility ATTN: Code D (Dickenson) Indian Head, MD 20640
1	Commander Naval Weapons Support Center ATTN: Code 502 Crane, IN 47522
1	Commander Naval Facilities Engineering Command ATTN: Code 04T5 Washington, DC 22360
1	Commander Naval Air Systems Command ATTN: AIR 532 Washington, DC 20360

<u>No. of Copies</u>	<u>Organization</u>	<u>No. of Copies</u>	<u>Organization</u>
2	Commander David W. Taylor Naval Ship Research & Development Center ATTN: Code 17 (Mr. Murray) Code 1/47 (Mr. Wilner) Bethesda, MD 20084-5000	2	Director Joint Strategic Target Planning Staff ATTN: JLTW TPTP Offutt AFB, Omaha, NE 68113
1	Commander Naval Ship R&D Center ATTN: Underwater Explosions Rsch Div (Mr. L.T. Butt) Portsmouth, VA 23709	1	HQ AFESC/RDC ATTN: Walter Buckholtz Tyndall AFB, FL 32403
2	Civil Engineering Laboratory Naval Construction Battalion Center ATTN: Code L31 Code L51 (Mr. Keenan) Port Hueneme, CA 93041	1	Director Office of Operational & Environmental Safety US Department of Energy Washington, DC 20545
3	HQ USAF (AFRIDO/AFRODXM/AFRDPM) WASH DC 20330	1	Director Office of Military Application US Department of Energy Washington, DC 20545
1	USAF Systems Command ATTN: IGFG Andrews Air Force Base Washington, DC 20334	1	US Department of Energy Albuquerque Operations Office ATTN: Operational Safety P.O. Box 5400 Albuquerque, NM 87115
1	Commander Air Force Rocket Propulsion Laboratory ATTN: Code AFRPL MKPA (Geisler) Edwards AFB, CA 93523	1	Director Pittsburgh Mining & Safety Research Center Bureau of Mines, Department of Interior 4800 Forbes Avenue Pittsburgh, PA 15213
3	Air Force Armament Laboratory ATTN: AFATL/DOIL (TIC) DLYV (Mr. McGuire) AFTAWC (OA) Eglin AFB, FL 32542-5438	1	Director Lawrence Livermore National Laboratory University of California P.O. Box 808 Livermore, CA 94550
1	Ogden ALC/MMWRE ATTN: Mr. Comins Hill Air Force Base, UT 84056	1	Director Los Alamos National Laboratory ATTN: Dr. J. Taylor P.O. Box 1663 Los Alamos, NM 87545
5	US Air Force ATTN: AFML (LNN/Nicholas; MBC/Schmidt) AFWAL/MLBC FTD/TQ Wright-Patterson AFB, OH 45433	1	Director Sandia National Laboratories ATTN: Div 6442 (von Riesenmann) P.O. Box 5800 Albuquerque, NM 87115
3	Director of Aerospace Safety ATTN: JDG/AFISC(SEVV) (COL McQueen) IDG/AFISC (SEW) (Gavitt) (SEV) (Gopher) Norton AFB, CA 92409	1	Director NASA-George C. Marshall Space Center Huntsville, AL 35812

<u>No. of Copies</u>	<u>Organization</u>	<u>No. of Copies</u>	<u>Organization</u>
2	Director NASA-Aerospace Safety Research & Data Institute Lewis Research Center 21000 Brook Park Road Cleveland, OH 44135	2	Kaman-AviDyne ATTN: Dr. N.P. Hobbs Mr. S. Criscione Northwest Industrial Park 83 Second Avenue Burlington, MA 01803
1	Director NASA-Scientific & Technical Information Facility P.O. Box 8757 Baltimore/Wash International Airport, MD 21240	3	Kaman-Nuclear ATTN: Dr. F.H. Shelton Dr. D. Sachs Dr. R. Keffe 1500 Garden of the Gods Road Colorado Springs, CO 80907
1	National Academy of Science ATTN: Mr. Groves 2101 Constitution Avenue, NW Washington, DC 20418	1	Knolls Atomic Power Laboratory ATTN: Dr. R.A. Powell Schenectady, NY 12309
1	Central Intelligence Agency OIR/DB/Standard GE47 HQ Washington, DC 20505	1	McDonnell Douglas Astronautics Western Division ATTN: Dr. Lea Cohen 5301 Bosla Avenue Huntington Beach, CA 92647
1	Applied Research Associates, Inc. 30 Diamond St., P.O. Box 548 ATTN: Mr. John H. Keefer Aberdeen, MD 21001	1	Physics International 2700 Merced Street San Leandro, CA 94577
1	Agbabian Associates ATTN: Dr. D.P. Reddy 250 N. Nash Street El Segundo, CA 90245	1	R&D Associates ATTN: Mr. John Lewis P.O. Box 9695 Marina del Rey, CA 90291
1	Black & Veatch, Engineers-Architects ATTN: Mr. H.D. Laverentz 1500 Meadow Lake Parkway Kansas City, MO 64114	1	R&D Associates ATTN: G.P. Ganong P.O. Box 9335 Albuquerque, NM 87119
1	Dr. Wilfred E. Baker Wilfred Baker Engineering P.O. Box 6477 San Antonio, TX 78209	2	The Boeing Company-Aerospace Div ATTN: Dr. Peter Grafton Dr. D. Strome (Mail Stop 8C-68) P.O. Box 3707 Seattle, WA 98124
1	Aeronautical Research Associates of Princeton, Inc. ATTN: Dr. Donaldson P.O. Box 2229 Princeton, NJ 08540	2	AVCO Corporation Structures & Mechanics Dept ATTN: Dr. William Broding Dr. J. Gilmore 201 Lowell Street Wilmington, MA 01887
1	J.G. Engineering Research Associates 3831 Menlo Drive Baltimore, MD 21215	1	Aerospace Corporation P.O. Box 92957 Los Angeles, CA 90009

<u>No. of Copies</u>	<u>Organization</u>	<u>No. of Copies</u>	<u>Organization</u>
1	General American Trans Corp General American Research Div ATTN: Dr. J.C. Shang 7449 N. Natchez Avenue Niles, IL 60648	1	Brown University Division of Engineering ATTN: Prof. R. Clifton Providence, RI 02912
1	Hercules, Inc. ATTN: Billings Brown P.O. Box 93 Magna, UT 84044	1	Florida Atlantic University Dept of Ocean Engineering ATTN: Prof. K.K. Stevens Boca Raton, FL 33432
1	Mason & Hanger-Silas Mason Co., Inc. Plantex Plant P.O. Box 647 Amarillo, TX 79117	1	Texas A&M University Dept of Aerospace Engineering ATTN: Dr. J.A. Stricklin College Station, TX 77843
1	Massachusetts Institute of Technology Aeroelastic & Structures Research Laboratory ATTN: Dr. E.A. Witmar Cambridge, MA 02139	1	University of Alabama ATTN: Dr. T.L. Cost P.O. Box 2908 Tuscaloosa, AL 35486
1	Monsanto Research Corporation Mound Laboratory ATTN: Frank Neff Miamisburg, OH 45342	1	University of Delaware Dept of Mechanical & Aerospace Engineering ATTN: Prof. J.R. Vinson Newark, DE 19711
1	Science Applications, Inc. Division 164, MST-3-2 1710 Goodridge Drive McLean, VA 22102	1	Denver Research Institute P.O. Box 10758 Denver, CO 80210 <u>Aberdeen Proving Ground</u>
2	Battelle Memorial Institute ATTN: Dr. L.E. Hulbert Mr. J.E. Backofen, Jr. 505 King Avenue Columbus, OH 43201	1	Cdr, USATHAMA, ATTN: AMXTH-TE
1	Georgia Institute of Tech ATTN: Dr. S. Atluri 225 North Avenue, NW Atlanta, GA 30332		
1	IIT Research Institute ATTN: Mrs. H. Napadensky 10 West 35th Street Chicago, IL 60616		
2	Southwest Research Institute ATTN: Dr. H.B. Abramson Dr. U.S. Lindholm 8500 Culebra Road San Antonio, TX 78228		
1	Agnes Scott College ATTN: Dr. A.L. Bowling Decatur, GA 30030		

INTENTIONALLY LEFT BLANK.

USER EVALUATION SHEET/CHANGE OF ADDRESS

This Laboratory undertakes a continuing effort to improve the quality of the reports it publishes. Your comments/answers to the items/questions below will aid us in our efforts.

1. BRL Report Number BRL-TR-3132 Date of Report AUGUST 1990

2. Date Report Received _____

3. Does this report satisfy a need? (Comment on purpose, related project, or other area of interest for which the report will be used.) _____

4. Specifically, how is the report being used? (Information source, design data, procedure, source of ideas, etc.) _____

5. Has the information in this report led to any quantitative savings as far as man-hours or dollars saved, operating costs avoided, or efficiencies achieved, etc? If so, please elaborate. _____

6. General Comments. What do you think should be changed to improve future reports? (Indicate changes to organization, technical content, format, etc.) _____

CURRENT
ADDRESS

Name

Organization

Address

City, State, Zip Code

7. If indicating a Change of Address or Address Correction, please provide the New or Correct Address in Block 6 above and the Old or Incorrect address below.

OLD
ADDRESS

Name

Organization

Address

City, State, Zip Code

(Remove this sheet, fold as indicated, staple or tape closed, and mail.)

-----FOLD HERE-----

DEPARTMENT OF THE ARMY

Director
U.S. Army Ballistic Research Laboratory
ATTN: SLCBR-DD-T
Aberdeen Proving Ground, MD 21005-5066
OFFICIAL BUSINESS



NO POSTAGE
NECESSARY
IF MAILED
IN THE
UNITED STATES

BUSINESS REPLY MAIL
FIRST CLASS PERMIT No 0001, APG, MD

POSTAGE WILL BE PAID BY ADDRESSEE

Director
U.S. Army Ballistic Research Laboratory
ATTN: SLCBR-DD-T
Aberdeen Proving Ground, MD 21005-9989

-----FOLD HERE-----

